01 Feb 2020

Effect of TiO2 Doping on Degradation Rate, Microstructure and Strength of Borate Bioactive Glass Scaffolds

Romina Shafaghi

Omar Rodriguez

Sunjeev Phull

Emil H. Schemitsch

et. al. For a complete list of authors, see https://scholarsmine.mst.edu/che_bioeng_facwork/1077

Recommended Citation

R. Shafaghi et al., "Effect of TiO2 Doping on Degradation Rate, Microstructure and Strength of Borate Bioactive Glass Scaffolds," *Materials Science and Engineering C*, vol. 107, article no. 110351, Elsevier, Feb 2020.

The definitive version is available at https://doi.org/10.1016/j.msec.2019.110351

Materials Science & Engineering C 107 (2020) 110351

Contents lists available at ScienceDirect

Materials Science & Engineering C

journal homepage: www.elsevier.com/locate/msec

Effect of TiO_2 doping on degradation rate, microstructure and strength of borate bioactive glass scaffolds

Romina Shafaghi[a,b], Omar Rodriguez[b,c], Sunjeev Phull[a,b], Emil H. Schemitsch[b,g], Paul Zalzal[e,f], Stephen D. Waldman[b,d], Marcello Papini[a,c], Mark R. Towler[a,b,c,*]

[a] Department of Biomedical Engineering, Ryerson University, Toronto M5B 2K3, Ontario, Canada
[b] Li Ka Shing Knowledge Institute, St Michael Hospital, Toronto M5B 1W8, Ontario, Canada
[c] Department of Mechanical Engineering, Ryerson University, Toronto M5B 2K3, Ontario, Canada
[d] Department of Chemical Engineering, Ryerson University, Toronto M5B 2K3, Ontario, Canada
[e] Oakville Trafalgar Memorial Hospital, Oakville L6J 3L7, Ontario, Canada
[f] Faculty of Health Sciences, Department of Surgery, McMaster University, Hamilton L8S 4L8, Ontario, Canada
[g] Department of Surgery, University of Western Ontario, London N68 4V2, Ontario, Canada

ARTICLE INFO

Keywords:
Scaffold
Borate bioactive glass
Titanium
Ion release
Compressive strength

ABSTRACT

A titanium-containing borate glass series based on the system (52-X) B_2O_3–12CaO–$6P_2O_5$–$14Na_2O$–16ZnO-$XTiO_2$ with X varying from 0, 5 and 15 mol% of TiO_2 incorporated, identified as BRT0, BRT1 and BRT3, respectively, were used in this study. Scaffolds (pore sizes, 165–230 μm and porosity, 53.51–69.51%) were prepared using a polymer foam replication technique. BRT3 scaffolds exhibited higher compressive strength (7.16 ± 0.22 MPa) when compared to BRT0 (6.02 ± 0.47 MPa) and BRT1 (5.65 ± 0.28 MPa) scaffolds with lower, or no, TiO_2 content. The solubility of the scaffolds decreased as the TiO_2 content increased up to 15 mol% when samples of each scaffold were immersed in DI water and the pH of all these extracts went up from 7.0 to 8.5 in 30 days. The cumulative ion release from the scaffolds showed significant difference with respect to TiO_2 content; addition of 5 mol% TiO_2 at the expense of borate (B_2O_3) decreased the ion release remarkably. Furthermore, it was found that for all three scaffolds, cumulative ion release increased with incubation time. The results indicate that the degradation rates and compressive strengths of borate bioactive glass scaffolds could be controlled by varying the amount of TiO_2 incorporated, confirming their potential as scaffolds in TKA and rTKA.

1. Introduction

Bone loss that compromises implant fixation is a challenge in both total knee arthroplasty (TKA) and revision total knee arthroplasty (rTKA). In 2016–17, more than 67,169 total knee arthroplasties (TKAs) were performed in Canada; a 15.5% increase over 2011–2012, and the total cost of these replacements was more than $ 0.5B [1]. The implants used to replace the joint can lead to the need for a revision total knee arthroplasty (rTKA) [2], as a result of infection (20.4%), wear and loosening of the implant (27.5%) and instability (14.2%) [1]. Revision TKAs are usually more complicated than primary TKAs due to the additional bone loss in the distal femur and proximal tibia [3].

The use of auto- or allografts in rTKAs is a common treatment for dealing with bone loss [4]. However, their limitations such as pain and blood loss associated with tissue harvesting (autografts), risk of infection and disease transmission (allografts) have necessitated the pursuit of synthetic scaffolds to facilitate the one million TKA bone graft procedures that are carried out worldwide each year [5,6]. Synthetic porous scaffolds can be made of metals, ceramics, polymers and composite materials (*eg.* graphene oxide - Mg alloys and nanodiamond – phospholipid/PLLA) [7–12]. However, some synthetic scaffolds carry the risk of toxicity and immunogenicity (polymer-based scaffolds) [13], cannot integrate with the surrounding environment (metal-based scaffolds) [14], or have low tensile strength (ceramics) [14]. Thus, the materials selected for preparation of the scaffolds are integral to their success.

Bioactive glasses are candidate materials for use as porous scaffolds in both primary TKA and rTKA, as they can influence the expression of osteogenic genes, and cell proliferation and differentiation by releasing ions into the surrounding environment [15,16]. However, the first macroporous scaffolds (45S5 Bioglass® [17,18]) fabricated using the replication method were brittle with low fracture toughness and

* Corresponding author. Department of Biomedical Engineering, Ryerson University, Toronto M5B 2K3, Ontario, Canada.
mtowler@ryerson.ca (M.R. Towler).

https://doi.org/10.1016/j.msec.2019.110351
Received 1 October 2018; Received in revised form 16 October 2019; Accepted 20 October 2019
Available online 23 October 2019
0928-4931/

Table 1
Bioactive glass compositions (mol %) [38].

Glass	B_2O_3	CaO	P_2O_5	Na_2O	ZnO	TiO_2
BRT0	52	12	6	14	16	0
BRT1	47	12	6	14	16	5
BRT3	37	12	6	14	16	15

compressive strength (0.27–0.42 MPa [19]) due to the poor sinterability of 45S5, which resulted in hollow struts in the scaffolds [20]. Furthermore, the tendency of such glasses to crystallize during thermal processing makes them less suitable as the result of a reduction in the rate of dissolution and bioactivity [21]. Therefore, the scaffolds not only were not suitable for load-bearing applications, but also they converted slowly and incompletely to HA in body fluid [22]. The mechanical properties and solubility of bioactive glass scaffolds can be improved by modifying the original composition of the glass and optimizing the sintering temperatures [23]. For example, glass 13–93 (54.6 mol. % SiO_2, 6.0 mol. % Na_2O, 22.1 mol. % CaO, 1.7 mol.% P_2O_5 and 7.7 mol.% MgO. Glass 13–93 is a bioactive glass with a wider sintering window that enables sintering before crystallization [24]. Recently, Brink et al. proposed the use of boro-silicate glasses, in which variable amounts of borate oxide are added to the silicate-based glass compositions to improve their bioactivity [25]. Borate bioactive glasses have lower chemical durability than silicate glasses, and they can thus convert more completely and quickly to an HA-like material, potentially reducing rehabilitation time for recipients of such implants [22,26,27]. The simplicity of fabrication and the ability to control the degradation rate in borate-based glasses make them good candidates for bone scaffolds. Furthermore, the compositional flexibility of these glasses makes it possible for them to act as a reservoir of ions (Zn, Ti, Cu, and Sr) that are known to both facilitate bone growth and inhibit bacterial proliferation [28,29].

It has been previously shown that titanium dioxide (TiO_2) is cytocompatible and has no significant effect on cell viability ($\leq$10 ppm) [30,31]. TiO_2 can also increase osteoblast differentiation and promote HA formation by contact with body fluid [32,33]. Furthermore, some studies have shown that osteoblasts produce growth factors known to stimulate angiogenesis (e.g. VEGF-A, FGF-2) [34,35]. As a result, TiO_2 indirectly stimulates angiogenesis by developing new blood vessels which help bone formation and bone repair. In addition, recent studies have shown that increasing the amount of TiO_2 incorporated in the glass can influence its role as a network forming (addition of up to 30 wt%) or a network modifying (up to 18 wt %) oxide in a glass which will consequently influence its solubility [36] and facilitate the modification of the degradation rate [37].

In the previous study, Rodriguez et al. designed a series of titanium-borate bioactive glasses for implant coatings [38]. Rodriguez showed introducing TiO_2 decreased the solubility of glass and consequently reduced Zn^{2+} release to undectable levels (BRT2 with 10 mol% of TiO_2), weakening the antibacterial effects [28]. while, further increase

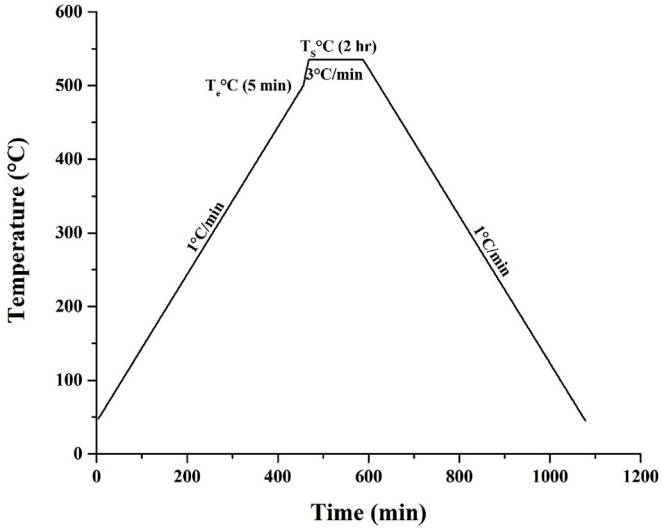

Fig. 2. Heat-treatment program for vaporizing (**Te**) the polyurethane blocks and sintering the borate-based glass scaffold (**Ts**).

Table 2
Differential scanning calorimetry of borate-based glass (DSC): glass transition (T_g), crystallization (T_x) and sintering (T_s) [38].

Glass	T_g (°C)	Tc (°C)	T_s (°C)
BRT0	521	603	515
BRT1	530	625	530
BRT3	523	633	535

of TiO_2 to 15 mol% led to an increase in the release of Zn^{2+} and antibacterial behavior (compared to 10 mol% of TiO_2) which is attributed to the occurrence of TiO_2 as a separate phase. As a result, in this study for preparing the scaffolds, glass compositions containing 0, 5 and 15 mol% of TiO_2 were selected [38].

The objective of this study was to evaluate the microstructure (pore size, porosity, pore interconnectivity), degradation behavior (solubility, ion release profile), pH, and compressive strength of borate-based bioactive glass scaffolds with varying TiO_2 content. In this study, in order to make scaffolds with large pores and high porosity, a polymer foam replication method was employed [39]. The as-fabricated scaffolds were immersed in de-ionized (DI) water in order to evaluate the degradation rate of the scaffolds as well as the pH change, and ultimately the effect of degradation on the compressive strength of the scaffolds.

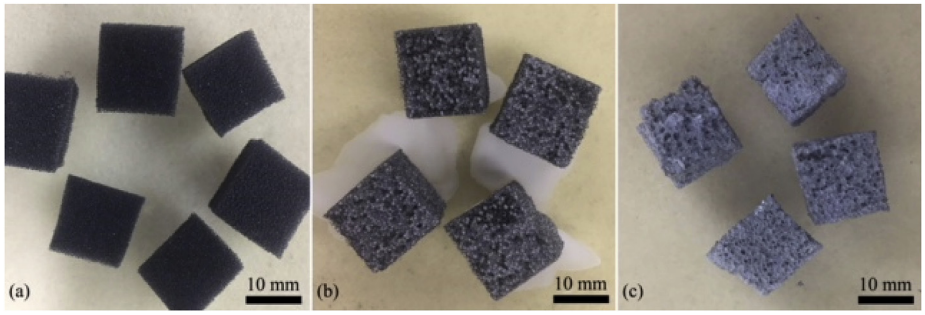

Fig. 1. Porous scaffold produced from borate-based glass (a) polyurethane foam (80ppi) (b) soaked samples in slurry (c) heat treated samples.

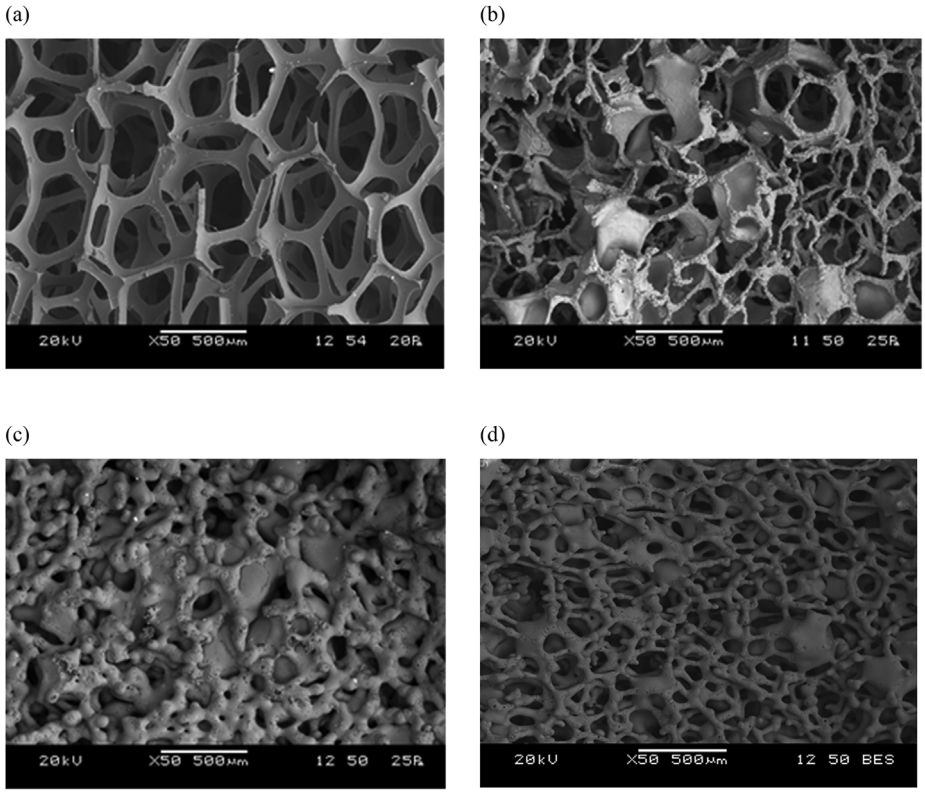

Fig. 3. Scanning electron microscopy images of (a) PU foam (80ppi), (b) BRT0 glass scaffold, (c) BRT1 glass scaffold and (d) BRT3 glass scaffold.

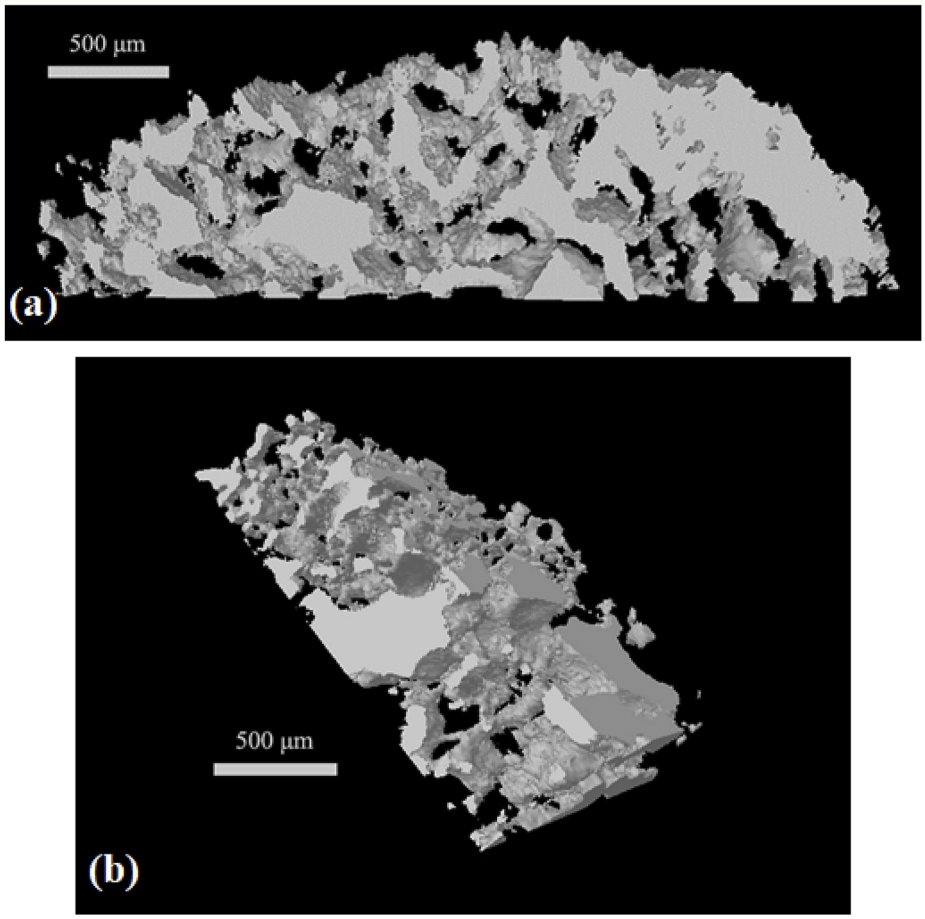

Fig. 4. Three-dimensional construction of BRT3 glass scaffold with open, interconnected macropores (a, b).

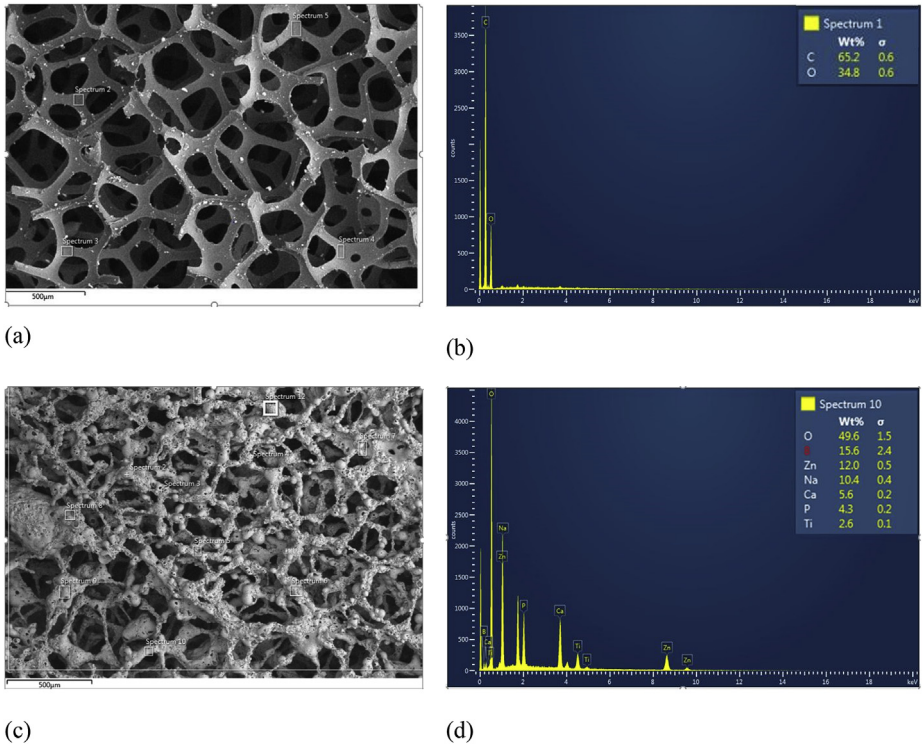

Fig. 5. A comparison of elemental composition of borate-glass scaffold with fresh foam. Fresh foam (a) and (b), glass scaffold (c) and (d). No carbon could be detected in the scaffold.

2. Materials and methods

2.1. Glass preparation

Since Rodriguez et al. successfully incorporated TiO_2 into borate glass structures and the glasses proved to be bioactive *in vitro*, it was these glass compositions that were used for scaffold preparation: BRT0, BRT1, and BRT3 (with 0, 5, 15 mol% TiO_2, respectively [38]. The chemical compositions of the three glasses are shown in Table 1.

The glasses were prepared by weighing out appropriate amounts of analytical grade reagents (Fisher Scientific, Ottawa, ON, Canada & Sigma-Aldrich, Oakville, ON, Canada), firing at 1200 °C for 1 h in silica crucibles, and shock quenching in cold water. The resulting frits were then ball-milled (Ball Mill PM 100, Retsch GmbH, Haan, Germany), and sieved to retrieve glass particles ≤ 20 μm.

2.2. Scaffold preparation

A polymer foam replication technique was used for preparing the scaffolds. Polyurethane (PU) foams with an open, interconnected macroporosity (80 ppi; Recticel Flexible Foams, Wetteren, Belgium) were cut in blocks (1.5 cm × 1.5 cm × 1.5 cm) and pre-treated in alcohol for 12 h then dipped in a slurry containing 42 wt% borate glass powder dispersed in ethanol (Fig. 1). The blocks of foams were immersed in the slurry. After 10 min the excess slurry was squeezed out of the blocks and the samples were dried overnight at room temperature. The dried samples were heated in a furnace as shown in Fig. 2.

The glass transition (T_g) and crystallization (T_x) temperatures for each glass were determined using differential scanning calorimetry (DSC). The sintering temperature (T_s) was chosen as the temperature when a bioglass scaffold was sintered (Table 2).

2.3. Structural characterization

The microstructure and the compositions of the as-fabricated glass scaffolds (n = 5 per composition) were investigated using scanning electron microscopy (SEM) equipped with an Energy-Dispersive Spectrometer (EDS) (JEOL, JSM-6380LV, Peabody, MA, USA). The pore interconnectivity of the scaffolds was evaluated using micro-CT (SkyScan 1174 X-ray, Kontich, Belgium) and CT-Volume software. The porosity of the scaffolds was assessed according to equations (1) and (2). First, the density of the cubic samples was calculated by measuring the mass and volume of the cubes as

$$\rho_{\text{scaffold}} = \frac{mass_{\text{scaffold}}}{volume_{\text{scaffold}}} \quad (1)$$

Then, the total porosity was determined as [40].

$$Total\ porosity = \left(1 - \frac{\rho_{\text{scaffold}}}{\rho_{\text{material}}}\right) \times 100 \quad (2)$$

where ρ_{scaffold} is the density of the scaffold and ρ_{material} is the density of the borate–based glass.

To calculate ρ_{material}, a cast of each glass was prepared and the resultant volume (using the Archimedes method) and weight were measured.

2.4. Compressive strength

The compressive strengths of the scaffolds (1.5 cm × 1.5 cm × 1.5 cm), as prepared (section 2.2), and after incubation in DI water for 1, 7, 14, and 30 days at 37 °C, were measured using a United Universal Tester (STM series, United Testing Systems, Inc. Huntington Beach CA USA) fitted with a 5000 N load cell at the cross head speed of 0.5 mm/min. The ratio of the scaffold mass to water volume was kept constant at 1 g per 100 cm^3 during the incubation [41], and the samples were dried in an oven at 37 °C overnight before testing them. Three samples of each glass (n = 5) at every incubation time were tested. The compressive strength σ_c was calculated as

$$\sigma_c = \frac{P}{A} \quad (3)$$

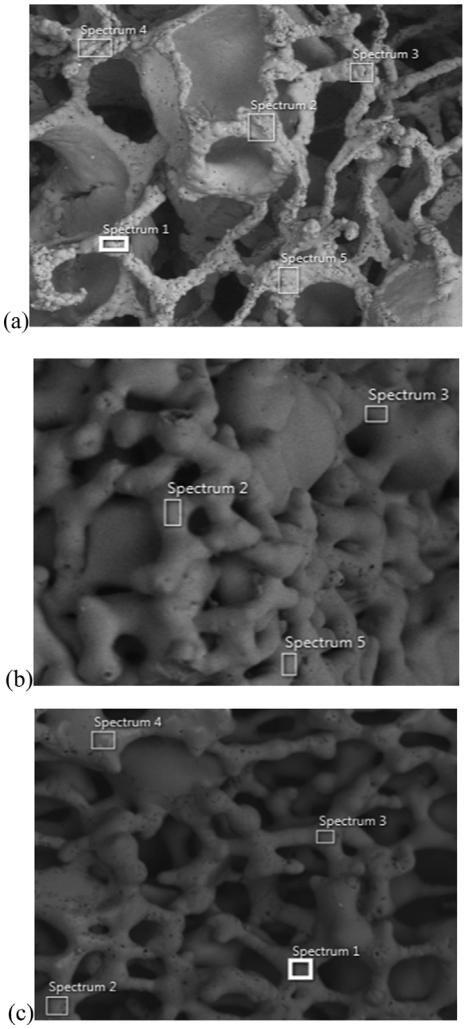

Mass %	BRT0
Oxygen (%)	46.22 ± 6.59
Boron (%)	17.22 ± 3.82
Zinc (%)	14.96 ± 12.97
Sodium (%)	7.1 ± 0.56
Calcium (%)	3.74 ± 0.59
Phosphorus (%)	2.2 ± 0.24
Titanium (%)	0.0 ± 0.0

Mass %	BRT1
Oxygen (%)	55.3 ± 1.9
Boron (%)	17.6 ± 2.48
Zinc (%)	0.66 ± 0.45
Sodium (%)	6.86 ± 0.67
Calcium (%)	0.96 ± 0.4
Phosphorus (%)	1.3 ± 0.3
Titanium (%)	1.32 ± 0.54

Mass %	BRT3
Oxygen (%)	49.3 ± 5.67
Boron (%)	11.3 ± 1.9
Zinc (%)	8.54 ± 4.01
Sodium (%)	7.58 ± 0.76
Calcium (%)	3.66 ± 0.79
Phosphorus (%)	2.46 ± 0.44
Titanium (%)	2.7 ± 1.2

Fig. 6. EDX compositional analysis of borate-glass scaffolds of three glasses BRT0, BRT1 and BRT3 (n = 5) (mean ± SD).

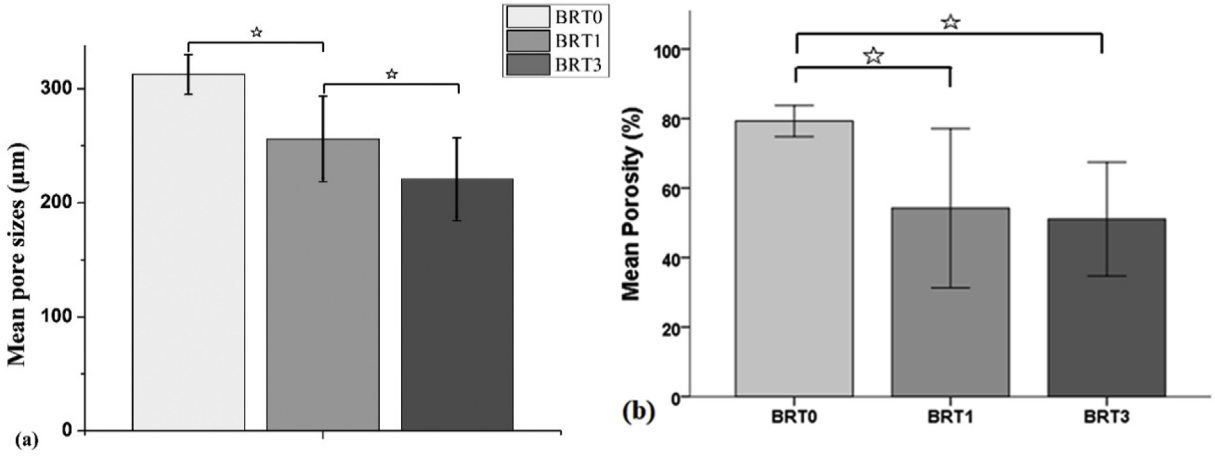

Fig. 7. Comparison of (a) Pore sizes and (b) porosity of BRT0, BRT1, and BRT3. Error bars indicate standard deviation from the mean (n = 5). Stars represent statistical significance between the samples ($p < 0.05$).

where P is the applied load at failure, and A is cross-sectional area of the sample.

2.5. In vitro degradation of the scaffolds

The degradation of the scaffolds was studied as a function of immersion in DI water with the samples maintained at a controlled temperature of 37 °C for 1, 7, 14 and 30 days. Samples (n = 5 per glass) were extracted from water after given times [42] dried and weighed (Denver Instrument, SI-114, NY, USA). The weight loss versus time was used to interpret the degradation kinetics, with weight loss calculated as

Table 3
Pore sizes and porosity of BRT0, BRT1 and BRT3 scaffolds compared to human trabecular bone (n = 5) (mean ± SD).

	Porosity (%)	Pore sizes (μm)
Trabecular bone	50 to more than 90 [44]	200 - 300 [45]
BRT0 scaffold	79.28 ± 2.59	312.8 ± 54.44
BRT1 scaffold	54.19 ± 13.22	255.95 ± 105.55
BRT3 scaffold	51.06 ± 8.19	220.62 ± 116.18

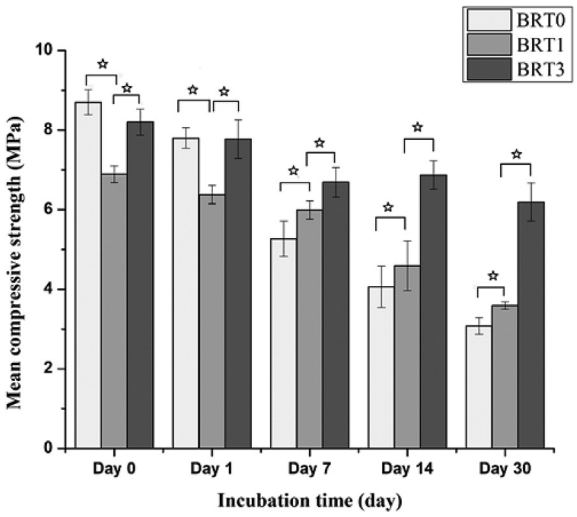

Fig. 8. Compressive strength as function of incubation time for BRT0, BRT1, and BRT3 scaffolds. Error bars indicate standard deviation from the mean (n = 5). Stars represent statistical significance between the samples ($p < 0.05$).

Table 4
Compressive strength of the scaffolds after 30 days compared to human trabecular bone (n = 5) (mean ± SD).

	Compressive strength (MPa)
Femur (trabecular bone) [46]	1.5–38*
BRT0 scaffolds	6.02 ± 2.27
BRT1 scaffolds	5.65 ± 1.35
BRT3 scaffolds	7.16 ± 1.22

*Depends on bone mineral density (BMD).

$$\Delta W_t = \left(\frac{W_0 - W_t}{W_0}\right) \times 100\% \quad (4)$$

where W_0 is the initial weight of the scaffold, and W_t is the weight of scaffold at time t after drying [43].

2.6. Determination of pH

Since the pH of the solution surrounding the scaffold affects the metabolism of adjacent cells and tissues, based on ASTM F2883-11, the pH of the solution containing the scaffold in deionized water was measured after 1, 7, 14 and 30 days using a pH meter (Versa Star Benchtop Meter VSTAR80, Thermo Fisher Scientific, MA, USA). The test was performed 5 times for each glass scaffold at each time point (1, 7, 14, 30 days). The results were compared to control samples with no scaffold (DI water in isolation).

2.7. Ion release

To investigate the ion release from the borate-based scaffolds, samples of each composition (n = 5) were incubated in DI water at 37 °C for 1, 7, 14, and 30 days. In order to determine the concentrations of Ti^{4+}, Ca^{2+}, Na^{+}, Zn^{2+}, PO_4^{3-} and BO_3^{3-} ions, calibration standards of 0.5,1, 2.5, 5 and 10 parts per million (ppm) for each of the mentioned ions were prepared from a 1000 ppm stock solution and then concentrations of the released ions in the suspensions were measured using inductively coupled plasma atomic emission spectroscopy (Optima 7300 DV ICP-OES, PerkinElmer, USA). The measurement was repeated five times for each glass scaffold, and for each time point, in order to assess scatter.

2.8. Statistical analysis

Statistical analysis was performed using SPSS software (IBM SPSS Statistics, version 24, NY, USA). A one-way and two-way ANOVA followed by Tukey's *post-hoc* test were used to determine the statistical significance of the differences between the measured compressive strengths, ion releases, pHs, pore sizes, porosities and weight losses, under different conditions. The differences between the groups were considered significant at $p \leq 0.05$. All results were presented as mean ± SD.

3. Results

3.1. Scanning electron microscopy (SEM) analysis of fabricated scaffolds

The effect of TiO_2 concentration on the pore sizes of the fabricated scaffolds was evaluated using SEM imaging (Fig. 3). Five scaffolds from each glass were imaged and the mean pore diameter distribution was determined from ten images for each scaffold. There was a ~29.5% decline in average pore size when the TiO_2 content increased from 0 to 15 mol%. As assessed by micro-CT the fabricated scaffold showed open and interconnected pores Fig. 4. The incomplete removal of excess slurry caused some clotted pores (Figs. 3 and 4).

3.2. Elemental composition analysis of fabricated scaffolds

EDS was used to ensure the incorporation of all the glass elements into the scaffold and vaporization of the polyurethane foam. The EDS traces confirmed that the polyurethane foam was fully vaporized, and the increase of TiO_2 at the expense of BO_3^{3-} for BRT1 and BRT3, as shown in Fig. 5 and Fig. 6.

3.3. Pore sizes and porosity

The pore sizes and porosities of the borate-based glass scaffolds as a function of TiO_2 content are shown in Fig. 7. The results showed that the porosity of the scaffolds depends on the content of TiO_2 in glass. The porosity of the scaffold decreased with increasing the amount of TiO_2. Also there was a significant difference in the pore sizes between BRT0 and BRT3 scaffolds ($p < 0.05$). As seen in Table 3, the porosity and pore sizes of the three groups of scaffolds were within the range of porosity and pore sizes of human trabecular bone [44].

3.4. Determination of compressive strength and elastic modulus

The compressive strengths of the fabricated borate-based glass scaffolds as a function of both incubation time in DI water and amount of TiO_2 incorporated are shown in Fig. 8. The results showed that the compressive strengths of the three groups of scaffolds generally decreased with incubation time. Moreover, after 30 days of incubation, the highest strength amongst the three groups was for the BRT3 scaffolds containing the highest amount of TiO_2. The compressive strengths of borate-based glass scaffolds are all with the range reported for human trabecular bone (Table 4).

The stress – strain curves of as-fabricated scaffolds under compression were also obtained. As seen in Fig. 9, during the initial stage of

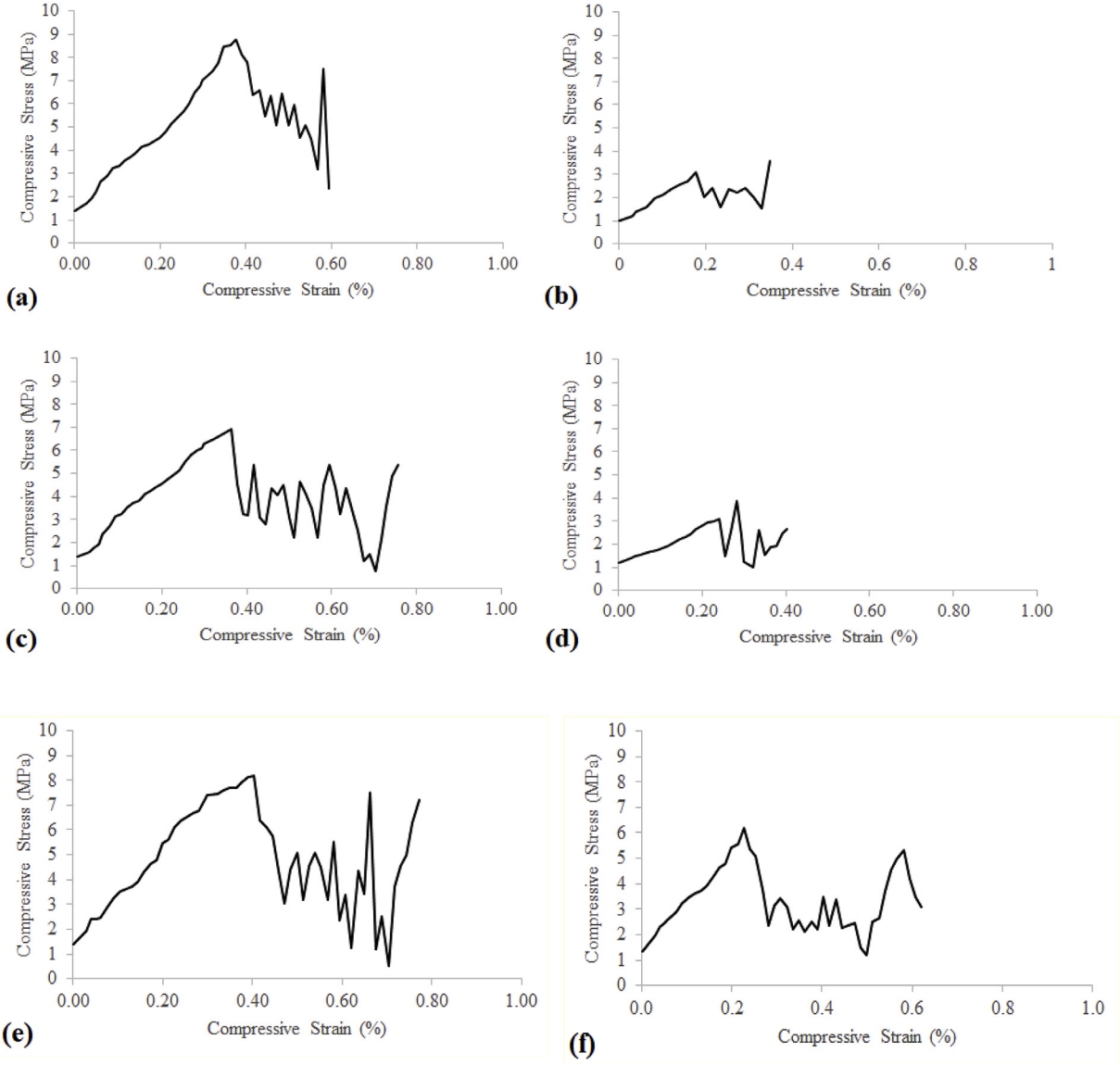

Fig. 9. Stress-strain responses of as fabricated scaffolds as function of incubation time (a) BRT0, (c) BRT1, (e) BRT3 scaffolds before incubation and (b) BRT0, (d) BRT1 and (f) BRT3 scaffolds at day 30.

compression the results show a behaviour typical to brittle materials with an almost linear trend. After the initial linear stage, the curves show a decrease in stress, which is believed to originate due to breakage of struts within the network. The progressive breaking of the struts after this point is manifested as fluctuations in the stress – strain curve. As the struts continue to fracture under compression, a continuous increase in strain is observed. The significant increase of stress at the end of the test can be related to accumulation of broken residues within the remaining pores and formation of a dense structure.

The slope of the initial linear stage of the curve was used to calculate the elastic modulus in each case. For BRT0, BRT1, and BRT3 scaffolds the elastic moduli were 1.78, 1.57, 1.92 GPa, respectively, before incubation, and 0.31, 0.19, 1.78 GPa at day 30. The elastic moduli of borate-based bioactive glass scaffolds are all with the range reported for human trabecular bone (0.1–5 GPa) [29].

3.5. Scaffold solubility

The mass loss of the scaffold was also studied as a function of incubation time. As can be seen in Fig. 10, the cumulative mass loss increased from day 1 to day 30 for all the scaffolds, with BRT0 scaffolds exhibiting the greatest solubility. A significant reduction in solubility can be observed as the amount of TiO_2 incorporated into the glass was increased.

3.6. Ion release from scaffolds

Ti^{4+}, Na^{+}, BO_3^{3-}, PO_4^{3-}, Zn^{2+}, and Ca^{2+} release from BRT0, BRT1, and BRT3 scaffolds are shown in Fig. 11. For all the bioactive scaffolds the cumulative ion release rate of Na^{+}, BO_3^{3-}, PO_4^{3-} and Ca^{2+} decreased with increasing Ti^{4+} concentration. BRT3 bioactive glass scaffolds containing 15% Ti^{4+} exhibited the lowest cumulative ion release compared to BRT0 and BRT1 glass scaffolds. Finally, the cumulative ion release rate increased with increased incubation time (Fig. 11)).

3.7. pH change

There was a significant difference in pH between BRT0 and BRT1, between BRT0 and BRT3, and between BRT1 and BRT3 glass scaffolds at days 0,1, 7 and 14 ($p < 0.05$). However, at 30 days all the extracts from the scaffolds (BRT0, BRT1 and BRT3) showed pH = ~8.5 Fig. 12.

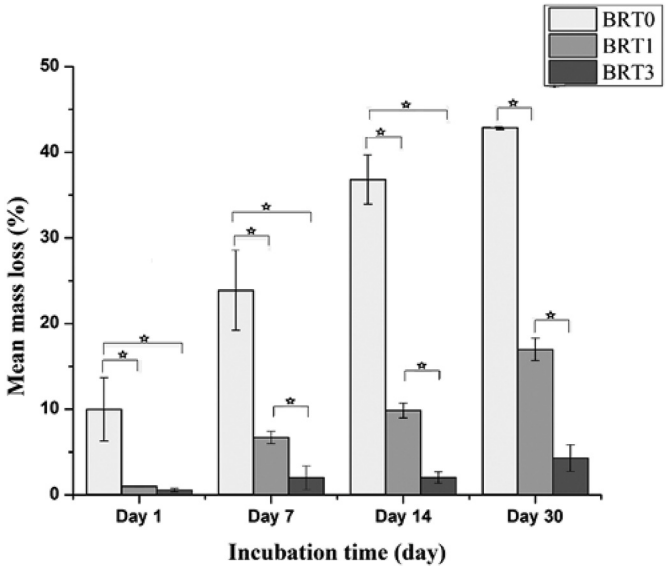

Fig. 10. Mass loss as a function of incubation time for BRT0, BRT1, and BRT3 glass scaffolds. Error bars indicate standard deviation from the mean (n = 5). Stars represent statistical significance between the samples ($p < 0.05$).

4. Discussion

The aim of this study was to determine the influence of TiO_2 incorporation on the microstructure, solubility, ion release, pH and compressive strength of borate bioactive glass scaffolds as a function of incubation time. As seen in Table 3, increasing TiO_2 content had a significant effect on the scaffolds in terms of porosity and the three bioactive glass scaffolds presented different porosities. Furthermore, a significant difference in the pore sizes between BRT0 and BRT3 scaffolds was observed, likely due to differences in TiO_2 content. Both the pore sizes and porosity of bioactive glass scaffolds have important roles in facilitating vascularization, migration and proliferation of osteoblasts [47]. Karageorgiou et al. showed that the minimum pore size for regenerating mineralized bone is about 100 µm and pores less than this induce the ingrowth of unmineralized bone tissue (fibrous) [48]. Thus, the microstructures of BRT0, BRT1, and BRT3 glass scaffolds developed within this study are suitable for bone regeneration and can potentially support bone ingrowth, vascularization, waste removal and nutrient delivery [48].

Wu et al. [49] indicated scaffolds with a higher porosity and a smaller pore size degrade more slowly than those with a lower porosity and a larger pore size. They attributed these results to the wall thickness and the surface area of the scaffold. Similar to their findings, in the present study, BRT3 with the smallest pore sizes of the three scaffolds, showed the least ion releases compared to BRT0 with the largest pore sizes. But, Wu et al. reported thicker walled porosity for larger pore sizes while in our study we found the opposite. Another criterion, surface area, reported by them was not determined in the present study for comparison. The probable cause of the ion release results is due to the chemical composition of the samples rather than due to the wall thickness effect as explained by Wu et al., and as seen in Fig. 11, ion release appears dependent on the content of Ti^{4+} in the glass. As Ti^{4+} content increased, cumulative Na^+, BO_3^{3-}, PO_4^{3-}, and Ca^{2+} ion release rates decreased. The increase in TiO_2 content causes the substitution of BO_3^{3-} with Ti^{4+} in B–O–B, and formation of B–O–Ti. TiO_2 ions have a small ionic radius and a large electric charge [37]. As a result, the network connectivity increases [37], which may explain the decrease of the cumulative ion release rate of the scaffolds with increasing Ti^{4+} content. However, as can be seen in Fig. 11a, the Ti^{4+} release itself did not follow the same trend for BRT3 scaffolds which had a higher Ti^{4+} content than BRT1, as expected, and the release rate of Ti^{4+} was also higher. Biocompatibility of titanium has been studied for decades [50], however since titanium is not present in body naturally, the role of titanium in bone formation and other pertinent metabolic changes is still controversial. Chan et al. showed that the interaction between titanium ions and cells caused inflammatory response [51], however Liao et al. showed the influence of titanium ions up to 10 ppm on osteoblast proliferation and differentiation [52]. Mine et al. investigated the effects of Ti^{4+} on the cell viability and cell differentiation of different cell lines, they showed Ti^{4+} concentrations ranged from 1 to 9 ppm had little biological effects on cells, including osteoblast-like MC3T3-E1, osteoblast-like RAW264.7 and epithelial cell-like GE-1 cells [53]. Ti^{4+} release from BRT1 and BRT3 in this study ranged from 0.025 to 0.35 ppm, and based on the literature the levels of Ti^{4+} were within therapeutic and non-toxic range [54]. Overall, the ion release profiles showed increasing trends with incubation time in all three groups of scaffolds. However, based on the results and literature, the levels of ions released from BRT3 were not toxic, especially in a dynamic environment, such as the human body [55,56].

The cumulative mass loss data in Fig. 10 shows that the substitution of BO_3^{3-} for TiO_2 in BRT1 and BRT3 glass scaffolds resulted in a decrease of the degradation rate compared to that observed with BRT0. TiO_2 is an intermediate oxide [57]; it can be a network modifier, which de-polymerizes the glass network and increases the concentration of non-bridging oxygen species (NBO) within the glass (increasing solubility); or a network former, which is involved in the structure of the glass network and increases the concentration of bridging oxygens; thereby decreasing solubility. By increasing the TiO_2 content of the glass, the solubility of the scaffolds decreased; BRT3, with the highest amount of TiO_2 (15 mol%), exhibited the least solubility (Fig. 10). A previous study [58] showed that increasing the TiO_2 content increases the structural stability of the glass because it changes the glass network structure. As a result, the decrease in solubility of the scaffolds might be due to the network former role of TiO_2 which can cause crystal formation. Thus, this significant difference in the degradation rate of the three scaffolds might be due to the presence of TiO_2 crystal phases in the scaffolds [38]. One of the most important factors for design and fabrication of a bone scaffold is the degradation rate. The mass loss rate of the scaffold should be close to the rate of bone formation in order to maintain the stability of the implant site. Thus, based on the cumulative mass loss results of this study, BRT3 scaffolds show the most promising results.

The Ti^{4+} content affects the pH of the DI water in our study, and, as can be seen in Fig. 12, there was a significant difference in pH between BRT0 and BRT1 and between BRT0 and BRT3 glass scaffolds at days 0 and 1. However, at 30 days, no significant differences were observed and all scaffolds exhibited a pH of ~8.5. The increase in pH in this study was the result of releasing the glass modifiers (Na^+, Ca^{2+}), coupled with the difference in acidity of BO_3^{3-}, a weak acid, and PO_4^{3-}. Galow et al. showed that increasing pH can be beneficial for proliferation and differentiation of bone cells [59]. Shen et al. demonstrated that the growth of osteoblasts occurs in more alkaline conditions than the physiological pH (7.4) [60]. Shen et al. showed that the optimum activity of osteoblasts occurs at approximately pH 8 [61]. Other studies revealed the stimulating and inhibitory effects of acidosis on osteoclast and osteoblast functions, respectively, resulting in bone resorption [62,63]. pH has been found to affect the balance of bone formation and resorption due to its effect on optimum activity of alkaline phosphatase (ALP), which plays a particularly important role in bone formation [64]. Harada et al. demonstrated the optimum pH for activity of ALP toward inorganic pyrophosphate, an inhibitor of mineral formation, was 8.5 [65]. pH here cannot realistically mimic a biological system, especially when the pH at an interface is the result of a dynamic system and there is a variation with time. As a result, an *in-vivo* study would be required to evaluate the effect of a dynamic environment on pH with the cell and tissue response to the values observed.

The compressive strength of the scaffolds increased with increasing

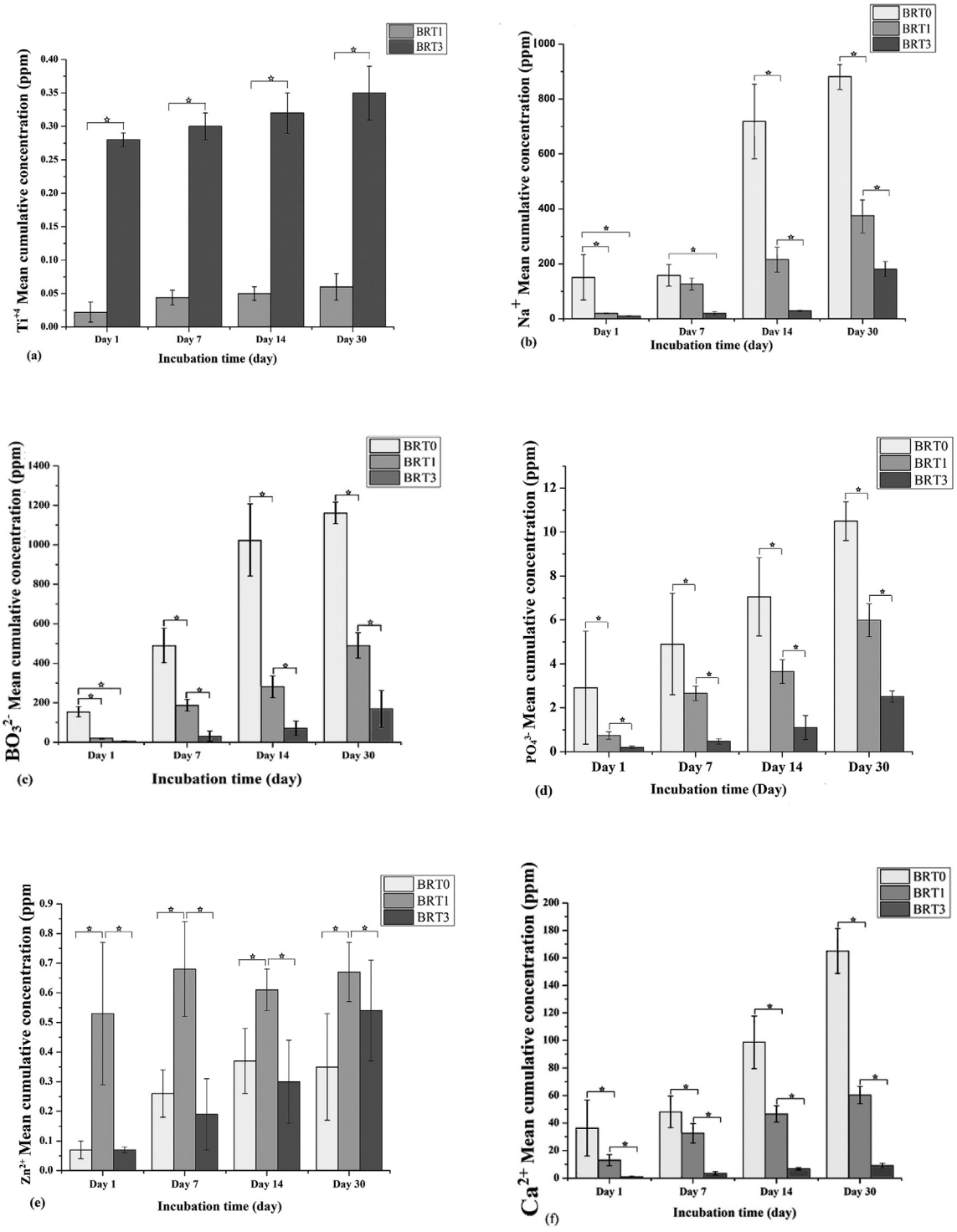

Fig. 11. Ion release profiles of (a) Ti^{4+}, (b) Na^{+}, (c) $BO_3{}^{2-}$, (d) $PO_4{}^{3-}$, (e) Zn^{2+}, and (f) Ca^{2+}. Error bars indicate standard deviation from the mean (n = 5). Stars show statistical significance between the samples ($p < 0.05$).

TiO_2 content; the compressive strength of BRT3 glass scaffolds reaching 10.56 ± 0.20 MPa at day 1. This increase might be attributed to the formation of crystalline phases in the glass structure [66] *via* addition of TiO_2. Also, the BRT3 glass scaffolds demonstrated the lowest strength and elastic modulus changes after 30 days, which is the result of its high TiO_2 content and its tendency to decrease the dissolution rate. The scaffold which had lower changes in compressive strength could be used in bone defects. However, borate bioactive glasses convert to HA in the human body and the mechanical properties of the scaffolds change with time. As a result, to provide further information, *in-vivo* mechanical tests of scaffolds with respect to time should be conducted to fully assess their use for load bearing applications.

5. Conclusions

Managing bone loss that can compromise implant fixation is a challenge in rTKAs. Fabricating scaffolds that not only support the implant, but also promote bone formation, could improve outcomes in

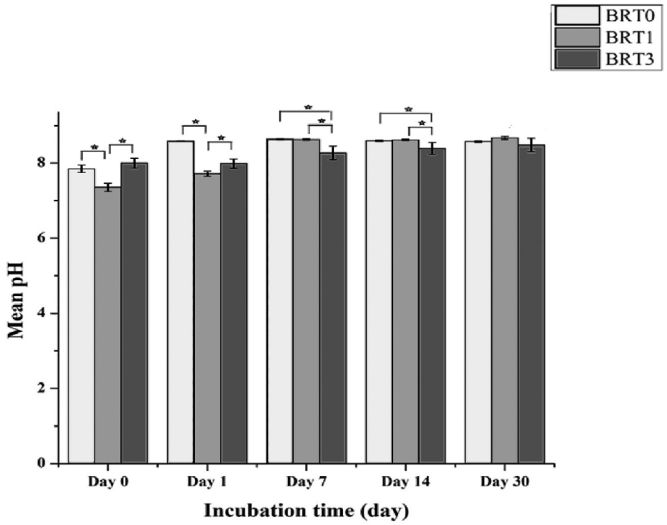

Fig. 12. pH changes as a function of incubation time of BRT0, BRT1, and BRT3 glass scaffolds in deionized water. Error bars indicate standard deviation from the mean (n = 5). Stars represent statistical difference between the samples ($p < 0.05$).

orthopedics. In this study, borate-based glass scaffolds containing different loadings of TiO_2 manufactured using the polymer foam replication technique were prepared. The scaffolds presented compressive strength and a microstructure close to human trabecular bone. The results obtained from ion release and pH in this work indicate that by incorporating TiO_2 in the glass system of the scaffolds, the degradation rate and the compressive strength of the scaffolds can be controlled. Also, the present study indicated that the amount of TiO_2 incorporated in the glass can influence the pore sizes and porosity of the scaffolds. Thus, making borate glass scaffolds containing TiO_2 *via* the replication method is a promising method for dealing with bone loss in both TKAs and rTKAs. However, additional *in-vitro* studies; including cell culture and antibacterial testing and *in-vivo* studies (animal trials) are required in order to evaluate the cytotoxic potential, biocompatibility and antibacterial activity of scaffolds in a controlled biological system and on a living subject.

Limitations of the study

The surface area of the scaffolds was not measured and so, whilst pore size and extent of porosity are reported, the influence of surface area is not known. Surface area would be expected to have an effect on degradation and will be reported in future studies.

Declaration of competing interest

The authors declare that they have no known competing financial interests or personal relationships that could have appeared to influence the work reported in this paper.

Acknowledgment

The authors would like to thank CIHR/NSERC-Collaborative Health Research Projects (356780-DAN) for the financial support.

References

[1] Hip and Knee Replacements in Canada, 2016-2017, Canadian Institute for Health Information, 2018.
[2] P.F. Sharkey, W.J. Hozack, R.H. Rothman, S. Shastri, S.M. Jacoby, Why are total knee arthroplasties failing today? Clin. Orthop. Relat. Res. 404 (2002) 7–13.
[3] P. Kempshall, H. Sharma, R. Morgan-Jones, (v) Revision total knee arthroplasty: complications, Orthop. Traumatol. 26 (2012) 95–111.
[4] T.P. Sculco, J.C. Choi, The role and results of bone grafting in revision total knee replacement, Orthop. Clin. N. Am. 29 (1998) 339–346.
[5] J.R. Jones, Reprint of: review of bioactive glass: from Hench to hybrids, Acta Biomater. 23 (2015) S53–S82.
[6] S. Wu, X. Liu, K.W. Yeung, C. Liu, X. Yang, Biomimetic porous scaffolds for bone tissue engineering, Mater. Sci. Eng. R Rep. 80 (2014) 1–36.
[7] C. Shuai, Y. Li, G. Wang, W. Yang, S. Peng, P. Feng, Surface modification of nanodiamond: toward the dispersion of reinforced phase in poly-l-lactic acid scaffolds, Int. J. Biol. Macromol. 126 (2019) 1116–1124.
[8] C. Shuai, B. Wang, Y. Yang, S. Peng, C. Gao, 3D honeycomb nanostructure-encapsulated magnesium alloys with superior corrosion resistance and mechanical properties, Compos. B Eng. 162 (2019) 611–620.
[9] K. Alvarez, H. Nakajima, Metallic scaffolds for bone regeneration, Materials 2 (2009) 790.
[10] L.-C. Gerhardt, A.R. Boccaccini, Bioactive glass and glass-ceramic scaffolds for bone tissue engineering, Materials 3 (2010) 3867–3910.
[11] X. Liu, P.X. Ma, Polymeric scaffolds for bone tissue engineering, Ann. Biomed. Eng. 32 (2004) 477–486.
[12] K. Rezwan, Q. Chen, J. Blaker, A.R. Boccaccini, Biodegradable and bioactive porous polymer/inorganic composite scaffolds for bone tissue engineering, Biomaterials 27 (2006) 3413–3431.
[13] E.J. Bergsma, F.R. Rozema, R.R. Bos, W.C. De Bruijn, Foreign body reactions to resorbable poly (L-lactide) bone plates and screws used for the fixation of unstable zygomatic fractures, J. Oral Maxillofac. Surg. 51 (1993) 666–670.
[14] An Introduction to Bioceramics, Imperial College Press, 2013.
[15] I.D. Xynos, A.J. Edgar, L.D. Buttery, L.L. Hench, J.M. Polak, Gene-expression profiling of human osteoblasts following treatment with the ionic products of Bioglass® 45S5 dissolution, J. Biomed. Mater. Res. 55 (2001) 151–157.
[16] J.Y. Sun, Y.S. Yang, J. Zhong, D.C. Greenspan, The effect of the ionic products of Bioglass® dissolution on human osteoblasts growth cycle in vitro, J. Tissue Eng. Regenerat. Med. 1 (2007) 281–286.
[17] L. Hench, H. Paschall, Histochemical responses at a biomaterial's interface, J. Biomed. Mater. Res. A 8 (1974) 49–64.
[18] L.L. Hench, The story of Bioglass®, J. Mater. Sci. Mater. Med. 17 (2006) 967–978.
[19] Q.Z. Chen, I.D. Thompson, A.R. Boccaccini, 45S5 Bioglass®-derived glass–ceramic scaffolds for bone tissue engineering, Topics in Tissue Engineering, vol. 27, (2006), pp. 2414–2425.
[20] F. Baino, S. Hamzehlou, S. Kargozar, Bioactive glasses: where are we and where are we going? J. Funct. Biomater. 9 (2018) 25.
[21] P. Li, Q. Yang, F. Zhang, T. Kokubo, The effect of residual glassy phase in a bioactive glass-ceramic on the formation of its surface apatite layerin vitro, J. Mater. Sci. Mater. Med. 3 (1992) 452–456.
[22] W. Huang, D.E. Day, K. Kittiratanapiboon, M.N. Rahaman, Kinetics and mechanisms of the conversion of silicate (45S5), borate, and borosilicate glasses to hydroxyapatite in dilute phosphate solutions, J. Mater. Sci. Mater. Med. 17 (2006) 583–596.
[23] M.E. Santocildes-Romero, A. Crawford, P.V. Hatton, R.L. Goodchild, I.M. Reaney, C.A. Miller, The osteogenic response of mesenchymal stromal cells to strontium--substituted bioactive glasses, J. Tissue Eng. Regenerat. Med. 9 (2015) 619–631.
[24] A. Nommeots-Nomm, J. Massera, Glass and glass-ceramic scaffolds: manufacturing methods and the impact of crystallization on in-vitro dissolution, Scaffolds Tissue Eng. Mater. Technol. Clin. Appl. (2017) 31.
[25] M. Brink, T. Turunen, R.P. Happonen, A. Yli-Urpo, Compositional dependence of bioactivity of glasses in the system Na2O-K2O-MgO-CaO-B2O3-P2O5-SiO2, J. Biomed. Mater. Res. A 37 (1997) 114–121.
[26] A. Yao, D. Wang, W. Huang, Q. Fu, M.N. Rahaman, D.E. Day, In vitro bioactive characteristics of borate-based glasses with controllable degradation behavior, J. Am. Ceram. Soc. 90 (2007) 303–306.
[27] W. Huang, M.N. Rahaman, D.E. Day, Conversion of bioactive silicate (45S5), borate, and borosilicate glasses to hydroxyapatite in dilute phosphate solution, Advances in Bioceramics and Biocomposites II, ceramic engineering and science proceedings, 2007, pp. 131–140.
[28] O. Rodriguez, W. Stone, E.H. Schemitsch, P. Zalzal, S. Waldman, M. Papini, et al., Titanium addition influences antibacterial activity of bioactive glass coatings on metallic implants, Heliyon 3 (2017) e00420.
[29] Q. Fu, E. Saiz, M.N. Rahaman, A.P. Tomsia, Bioactive glass scaffolds for bone tissue engineering: state of the art and future perspectives, Mater. Sci. Eng. C 31 (2011) 1245–1256.
[30] J.Y. Wang, B.H. Wicklund, R.B. Gustilo, D.T. Tsukayama, Titanium, chromium and cobalt ions modulate the release of bone-associated cytokines by human monocytes/macrophages in vitro, Biomaterials 17 (1996) 2233–2240.
[31] W.Q. Zhu, P.P. Ming, J. Qiu, S.Y. Shao, Y.J. Yu, J.X. Chen, et al., Effect of titanium ions on the Hippo/YAP signaling pathway in regulating biological behaviors of MC3T3-E1 osteoblasts, J. Appl. Toxicol. 38 (2018) 824–833.
[32] M. Hashimoto, S. Kitaoka, H. Kanetaka, Effect of surface charge of TiO2 particles on hydroxyapatite formation in simulated body fluid, Adv. Powder Technol. 27 (2016) 2409–2415.
[33] A.L. Raines, R. Olivares-Navarrete, M. Wieland, D.L. Cochran, Z. Schwartz, B.D. Boyan, Regulation of angiogenesis during osseointegration by titanium surface microstructure and energy, Biomaterials 31 (2010) 4909–4917.
[34] D.S. Wang, M. Miura, H. Demura, K. Sato, Anabolic effects of 1, 25-dihydroxyvitamin D3 on osteoblasts are enhanced by vascular endothelial growth factor produced by osteoblasts and by growth factors produced by endothelial cells, Endocrinology 138 (1997) 2953–2962.
[35] M.M. Hurley, C. Abreu, G. Gronowicz, H. Kawaguchi, J. Lorenzo, Expression and

regulation of basic fibroblast growth factor mRNA levels in mouse osteoblastic MC3T3-E1 cells, J. Biol. Chem. 269 (1994) 9392–9396.
[36] L.M. Placek, T.J. Keenan, Y. Li, C. Yatongchai, D. Pradhan, D. Boyd, et al., Investigating the effect of TiO2 on the structure and biocompatibility of bioactive glass, J. Biomed. Mater. Res. B Appl. Biomater. 104 (2016) 1703–1712.
[37] A.W. Wren, A. Coughlan, C.M. Smith, S.P. Hudson, F.R. Laffir, M.R. Towler, Investigating the solubility and cytocompatibility of CaO–Na2O–SiO2/TiO2 bioactive glasses, J. Biomed. Mater. Res. A 103 (2015) 709–720.
[38] O. Rodriguez, D.J. Curran, M. Papini, L.M. Placek, A.W. Wren, E.H. Schemitsch, et al., Characterization of silica-based and borate-based, titanium-containing bioactive glasses for coating metallic implants, J. Non-Cryst. Solids 433 (2016) 95–102.
[39] Q. Fu, M.N. Rahaman, B.S. Bal, R.F. Brown, D.E. Day, Mechanical and in vitro performance of 13–93 bioactive glass scaffolds prepared by a polymer foam replication technique, Acta Biomater. 4 (2008) 1854–1864.
[40] Q.L. Loh, C. Choong, Three-dimensional scaffolds for tissue engineering applications: role of porosity and pore size, Tissue Eng. B Rev. 19 (2013) 485–502.
[41] X. Liu, M.N. Rahaman, G.E. Hilmas, B.S. Bal, Mechanical properties of bioactive glass (13-93) scaffolds fabricated by robotic deposition for structural bone repair, Acta Biomater. 9 (2013) 7025–7034.
[42] D. Bellucci, V. Cannillo, A. Sola, A new highly bioactive composite for scaffold applications: a feasibility study, Materials 4 (2011) 339–354.
[43] Q. Fu, M.N. Rahaman, H. Fu, X. Liu, Silicate, borosilicate, and borate bioactive glass scaffolds with controllable degradation rate for bone tissue engineering applications. I. preparation and in vitro degradation, J. Biomed. Mater. Res. A 95 (2010) 164–171.
[44] A. Wall, T. Board, The compressive behavior of bone as a two-phase porous structure, Classic Papers in Orthopaedics, Springer, 2014, pp. 457–460.
[45] T. Doktor, J. Valach, D. Kytyr, O. Jiroušek, Pore Size Distribution of Human Trabecular Bone - Comparison of Intrusion Measurements with Image Analysis, (2011).
[46] S. Khan, R. Warkhedkar, A. Shyam, Human bone strength evaluation through different mechanical tests, Int. J. Curr. Eng. Technol. 2 (2014) 539–543.
[47] C.M. Murphy, M.G. Haugh, F.J. O'Brien, The effect of mean pore size on cell attachment, proliferation and migration in collagen–glycosaminoglycan scaffolds for bone tissue engineering, Biomaterials 31 (2010) 461–466.
[48] V. Karageorgiou, D. Kaplan, Porosity of 3D biomaterial scaffolds and osteogenesis, Biomaterials 26 (2005) 5474–5491.
[49] L. WU, J. DING, Effects of porosity and pore size on in vitro degradation of three-dimensional porous poly (D, L-lactide-co-glycolide) scaffolds for tissue engineering, J. Biomed. Mater. Res. A 75 (2005) 767–777.
[50] B. Kasemo, Biocompatibility of titanium implants: surface science aspects, J. Prosthet. Dent 49 (1983) 832–837.
[51] E.P. Chan, A. Mhawi, P. Clode, M. Saunders, L. Filgueira, Effects of titanium (iv) ions on human monocyte-derived dendritic cells, Metallomics 1 (2009) 166–174.
[52] H. Liao, T. Wurtz, J. Li, Influence of titanium ion on mineral formation and properties of osteoid nodules in rat calvaria cultures, J. Biomed. Mater. Res. 47 (1999) 220–227.
[53] Y. Mine, S. Makihira, H. Nikawa, H. Murata, R. Hosokawa, A. Hiyama, et al., Impact of titanium ions on osteoblast-, osteoclast-and gingival epithelial-like cells, J. Prosthodont. Res. 54 (2010) 1–6.
[54] H.C. Liu, W.H.S. Chang, F.H. Lin, K.H. Lu, Y.H. Tsuang, J.S. Sun, Cytokine and prostaglandin E2 release from leukocytes in response to metal ions derived from different prosthetic materials: an in vitro study, Artif. Organs 23 (2004).
[55] S.B. Jung, D.E. Day, R.F. Brown, L.F. Bonewald, Potential toxicity of bioactive borate glasses in-vitro and in-vivo, Advances in Bioceramics and Porous Ceramics V, 2012, pp. 65–74.
[56] B. Kramer, F.F. Tisdall, The distribution of sodium, potassium, calcium, and magnesium between the corpuscles and serum of human blood, J. Biol. Chem. 53 (1922) 241–252.
[57] D.S. Brauer, N. Karpukhina, R.V. Law, R.G. Hill, Effect of TiO2 addition on structure, solubility and crystallisation of phosphate invert glasses for biomedical applications, J. Non-Cryst. Solids 356 (2010) 2626–2633.
[58] N.J. Lakhkar, I.-H. Lee, H.-W. Kim, V. Salih, I.B. Wall, J.C. Knowles, Bone formation controlled by biologically relevant inorganic ions: role and controlled delivery from phosphate-based glasses, Adv. Drug Deliv. Rev. 65 (2013) 405–420.
[59] A.-M. Galow, A. Rebl, D. Koczan, S.M. Bonk, W. Baumann, J. Gimsa, Increased osteoblast viability at alkaline pH in vitro provides a new perspective on bone regeneration, Biochem. Biophys. Rep. 10 (2017) 17–25.
[60] Y. Shen, W. Liu, K. Lin, H. Pan, B.W. Darvell, S. Peng, et al., Interfacial pH: a critical factor for osteoporotic bone regeneration, Langmuir 27 (2011) 2701–2708.
[61] Y. Shen, W. Liu, C. Wen, H. Pan, T. Wang, B.W. Darvell, et al., Bone regeneration: importance of local pH—strontium-doped borosilicate scaffold, J. Mater. Chem. 22 (2012) 8662–8670.
[62] D.A. Bushinsky, Acid-base imbalance and the skeleton, Eur. J. Nutr. 40 (2001) 238–244.
[63] A. Brandao-Burch, J. Utting, I. Orriss, T. Arnett, Acidosis inhibits bone formation by osteoblasts in vitro by preventing mineralization, Calcif. Tissue Int. 77 (2005) 167–174.
[64] M. Ross, J. Ely, J. Archer, Alkaline phosphatase activity and pH optima, J. Biol. Chem. 192 (1951) 561–568.
[65] M. Harada, N. Udagawa, K. Fukasawa, B. Hiraoka, M. Mogi, Inorganic pyrophosphatase activity of purified bovine pulp alkaline phosphatase at physiological pH, J. Dent. Res. 65 (1986) 125–127.
[66] G. Kaur, O.P. Pandey, K. Singh, D. Homa, B. Scott, G. Pickrell, A review of bioactive glasses: their structure, properties, fabrication and apatite formation, J. Biomed. Mater. Res. A 102 (2014) 254–274.